

An analysis of the strains in the embossing stage of the deep drawing process

Citation for published version (APA):

Minghai, G., & Hoogenboom, S. M. (1991). *An analysis of the strains in the embossing stage of the deep drawing process*. (TH Eindhoven. Afd. Werktuigbouwkunde, Vakgroep Produktietechnologie : WPB; Vol. WPA1147). Technische Universiteit Eindhoven.

Document status and date:

Published: 01/01/1991

Document Version:

Publisher's PDF, also known as Version of Record (includes final page, issue and volume numbers)

Please check the document version of this publication:

- A submitted manuscript is the version of the article upon submission and before peer-review. There can be important differences between the submitted version and the official published version of record. People interested in the research are advised to contact the author for the final version of the publication, or visit the DOI to the publisher's website.
- The final author version and the galley proof are versions of the publication after peer review.
- The final published version features the final layout of the paper including the volume, issue and page numbers.

[Link to publication](#)

General rights

Copyright and moral rights for the publications made accessible in the public portal are retained by the authors and/or other copyright owners and it is a condition of accessing publications that users recognise and abide by the legal requirements associated with these rights.

- Users may download and print one copy of any publication from the public portal for the purpose of private study or research.
- You may not further distribute the material or use it for any profit-making activity or commercial gain
- You may freely distribute the URL identifying the publication in the public portal.

If the publication is distributed under the terms of Article 25fa of the Dutch Copyright Act, indicated by the "Taverne" license above, please follow below link for the End User Agreement:

www.tue.nl/taverne

Take down policy

If you believe that this document breaches copyright please contact us at:

openaccess@tue.nl

providing details and we will investigate your claim.

✓ AN ANALYSIS OF THE STRAINS IN THE
EMBOSSING STAGE OF THE DEEP
DRAWING PROCESS

ir. Guo Minghai
ir. S.M.Hoogenboom

August 1991
IOPM-D 013

WPA 1147 A

CONTENTS

| | |
|---|--------|
| NOTATION AND REFERENCE | (1) |
| I. INTRODUCTION | (3) |
| II. MODELLING AND THE ANALYSIS | (3) |
| 2.1 Introduction | (3) |
| 2.2 The Total Deformation Energy | (5) |
| III. RESULTS AND CONCLUSIONS | (11) |
| APPENDIX | (17) |
| A. Derivation of u | (17) |
| B. Derivation of dv , $1 + \frac{s_2^*}{\rho_P^*}$, and $1 + \frac{s_4^*}{\rho_D^*}$ | (18) |
| C. Uniaxial Stress in Region 3 | (20) |

NOTATION AND REFERENCE

Notation

| | |
|-----------------|--|
| W | the total deformation energy in the whole sheet; |
| W_j | the deformation energy in the j th area ($j=1,2,3,4,5$); |
| W_s | the special deformation energy; |
| C, n | characteristic stress, strain hardening exponent; |
| r, φ, z | the principal directions of the coordinate system; |
| α | the angle containing the arc in the flange touched by the punch; |
| r_i | the inner radius of the flange, which is $r_D + \rho_D$; |
| β_0 | the initial ratio of the outer and the inner radii of the flange, or r_{u0}/r_i ; |
| u | the displacement of the punch; |
| r_j | the initial radii of the points A, B, C, and D, or the radii of the points $A_0, B_0, C_0,$ and D_0 ($j=1,2,3,4$); |
| r_u | the momentary radius of the edge of the flange; |
| s_j | the thicknesses of the j th area; |
| ρ_1 | the local coordinate used in the punch chamfering area; |
| ρ_2 | the local coordinate used in the die chamfering area; |
| t | the gap between the punch and the die; |
| r_P | the radius of the punch; |
| ρ_D | the chamfering radius of the die; |
| ρ_P | the chamfering radius of the punch; |

Also, the following dimensionless quantities are defined:

$$W^* = \frac{W}{C\pi r_i^2 s_0};$$

$$W_j^* = \frac{W_j}{C\pi r_i^2 s_0} \quad (j=1,2,3,4,5);$$

$$W_s^* = \frac{W_s}{C}$$

$$r_j^* = \frac{r_j}{r_i} \quad (j=1,2,3,4);$$

$$s_0^* = \frac{s_0}{r_i};$$

$$u^* = \frac{u}{r_i};$$

$$r_P^* = \frac{r_P}{r_i};$$

$$s_j^* = \frac{s_j}{s_0} \quad (j=1,2,3,4);$$

$$\rho_P^* = \frac{\rho_P}{s_0};$$

$$\rho_D^* = \frac{\rho_D}{s_0};$$

$$t^* = \frac{t}{s_0};$$

$$\rho_1^* = \frac{\rho_1}{\rho_P};$$

$$\rho_2^* = \frac{\rho_2}{\rho_P}.$$

Reference

- [1] M.Kessels, Eindige Elementen Simulatie van het Dieptrekprocede,
Afstudeerverslag TUE, WPA 1163, 1991.

I. INTRODUCTION

The first phase of the deep-drawing process, embossing, is of importance for the critical deepdrawing force which occurs later in the process.

Particularly the stretch-bending which takes place near the punchradius is of major concern because this is the area where necking and eventually tearing occurs.

In this report the analysis of the strains in the flange during the embossing stage will be given based on the minimization of the total deformation energy.

II. MODELLING FOR THE ANALYSIS

2.1 Introduction

In this analysis, the following assumptions are applied:

___ r, φ , and z (see fig.2.1) are the principal directions;

___ the behaviour of the material is isotropic;

___ the process is axisymmetric;

___ plane stress is assumed, or $\sigma_z=0$;

___ friction and the deformations of the punch and die are neglected;

___ furthermore five areas can be distinguished (see Fig.2.1):

Area 1. the inner circle contacted with the surface of the punch;

Area 2. the fillet part contacted with the punch radius;

- Area 3. the straight contacted with neither the punch nor the die;
- Area 4. the fillet area contacted with the die radius;
- Area 5. the plane outer ring contacted with the upper surface of the die.

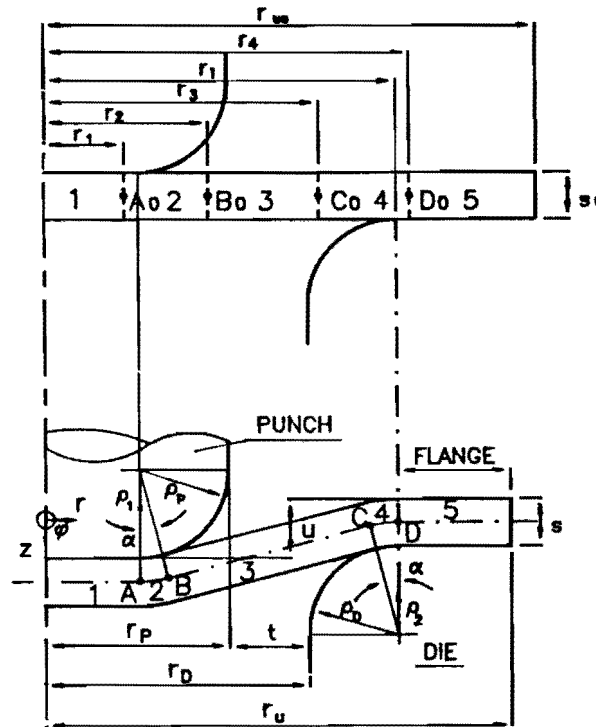


Fig.2.1 The Flange in the Deep-Drawing Process

The way the areas are described above they are located in the current position of the flange, where the material points A , B , C and D indicate the boundaries between the areas. The initial position of these points is given by A_0 (radius r_1), B_0 (radius r_2), C_0 (radius r_3) and D_0 (radius r_4).

The assumption of a simple deformation model for each area, among others a straight strain path, leads to the derivation of the total effective strain $\bar{\epsilon}_j$ ($j=1,2,3,4,5$). Then the specific deformation energy can be derived according to

$$W_s(\bar{\epsilon}_j) = \frac{C}{n+1} [(\bar{\epsilon}_j + \bar{\epsilon}_0)^{n+1} - \bar{\epsilon}_0^{n+1}] \quad (2.1)$$

For the deformation energy in the j th region, it follows

$$W_j = \int W_s(\bar{\epsilon}_j) \cdot dv \quad (2.2)$$

and for the total deformation energy, summation is applied

$$W = \sum_1^5 W_j \quad (2.3)$$

In this equation the initial position of the material points (r_1 until r_4) can be regarded as free parameters, the determination of which is realized by optimization.

2.2 The Total Deformation Energy

The relation between the displacement from the punch and the angle α (see Fig.2.1) is given by (Appendix A)

$$u = (r_i - r_D + \rho_P) \tan \alpha + (\rho_D + \rho_P + s_0) \cdot \frac{\cos \alpha - 1}{\cos \alpha} \quad (2.4)$$

where only for the derivation of this relation, the assumption is made that the change of the thickness of the sheet is ignorable, or $s_j = s_0$ ($j=1,2,3,4,5$). The dimensionless expression of Eq.(2.4) becomes

$$u^* = (1 - r_D^* + \rho_P^* s_0^*) \tan \alpha + s_0^* (\rho_D^* + \rho_P^* + 1) \cdot \frac{\cos \alpha - 1}{\cos \alpha} \quad (2.5)$$

In the following the deformation energy for each region is determined.

2.2.1 Area 1

In this area, since $\sigma_r = \sigma_\varphi$ and $\sigma_z = 0$, it yields

$$\epsilon_r = \epsilon_\varphi = -\frac{1}{2} \epsilon_z \quad (2.6)$$

thus,

$$\begin{aligned} \bar{\epsilon}_1 &= 2 |\epsilon_r| \\ &= 2 \left| \ln \frac{r_P - \rho_P}{r_1} \right| \end{aligned} \quad (2.7)$$

Using the dimensionless quantities gives

$$\bar{\epsilon}_1 = 2 \left| \ln \frac{r_P^* - \rho_P^* s_0^*}{r_1^*} \right| \quad (2.8)$$

Therefore, the deformation energy in Area 1 by Eq.(2.2) becomes

$$W_1 = W_s(\bar{\epsilon}_1) \cdot \pi r_1^2 \cdot s_0 \quad (2.9)$$

and its dimensionless expression is

$$W_1^* = W_s^*(\bar{\epsilon}_1) \cdot r_1^{*2} \quad (2.10)$$

2.2.2 Area 2

In this area, the effective strain is determined by the strain due to stretching-bending ϵ_{α_2} and the circumferential strain ϵ_{φ^2} . The first one is

$$\epsilon_{\alpha_2} = \ln \frac{\alpha \rho_1}{r_2 - r_1} \quad (2.11)$$

or dimensionless

$$\epsilon_{\alpha_2} = \ln \frac{\alpha \rho_1^* \rho_P^* s_0^*}{r_2^* - r_1^*} \quad (2.12)$$

The circumferential strain in this area can be derived by taking the mean strain of those in the points A and B. They are

$$\epsilon_{\varphi A} = \ln \frac{r_P - \rho_P}{r_1} \quad (2.13)$$

and

$$\epsilon_{\varphi B} = \ln \frac{r_P - \rho_P + \rho_1 \sin \alpha}{r_2} \quad (2.14)$$

Applying the mean value for the whole area gives

$$\epsilon_{\varphi^2} = \frac{1}{2} \ln \frac{(r_P - \rho_P)(r_P - \rho_P + \rho_1 \sin \alpha)}{r_1 r_2} \quad (2.15)$$

that is,

$$\epsilon_{\varphi^2} = \frac{1}{2} \ln \frac{(r_P^* - \rho_P^* s_0^*)(r_P^* - \rho_P^* s_0^* + \rho_1^* \rho_P^* s_0^* \sin \alpha)}{r_1^* r_2^*} \quad (2.16)$$

Thus, the effective strain in this area becomes

$$\bar{\epsilon}_2 = \frac{2}{\sqrt{3}} \cdot \sqrt{\epsilon_{\alpha_2}^2 + \epsilon_{\varphi_2}^2 + \epsilon_{\alpha_2} \cdot \epsilon_{\varphi_2}} \quad (2.17)$$

With the effective strain, the deformation energy of this area is

$$W_2 = \int W_s(\bar{\epsilon}_2) dv \quad (2.18)$$

where the volume element (see Appendix B)

$$dv = \rho_1 \left(\alpha r_P - \alpha \rho_P + 2\rho_1 \sin^2 \frac{\alpha}{2} \right) \cdot d\rho_1 \quad (2.19)$$

To ensure volume invariance, the integration of Eq.(2.18) must take place over the current thickness of the sheet s_2 , that is,

$$W_2 = \int_{\rho_P}^{\rho_P + s_2} W_s(\bar{\epsilon}_2) \cdot \rho_1 \left(\alpha r_P - \alpha \rho_P + 2\rho_1 \sin^2 \frac{\alpha}{2} \right) \cdot d\rho_1 \quad (2.20)$$

and dimensionless

$$W_2^* = 2\rho_P^* s_0^* \int_1^{1 + \frac{s_2^*}{\rho_P^*}} W_s^*(\bar{\epsilon}_2) \cdot \rho_1^* \left(\alpha \frac{r_P^*}{\rho_P^* s_0^*} - \alpha + 2\rho_1^* \sin^2 \frac{\alpha}{2} \right) \cdot d\rho_1^* \quad (2.21)$$

where the upper limitation of this integration $1 + \frac{s_2^*}{\rho_P^*}$ is determined in Appendix B.

2.2.3 Area 3

Assuming this area straight there is a uniaxial stress condition in the 1-direction (see Appendix C), thus the effective strain equals the natural strain in 1-direction, that is (see Appendix A)

$$\bar{\epsilon}_3 = \left| \ln \frac{r_1 - r_P + \rho_P - (\rho_P + \rho_D + s_0) \sin \alpha}{(r_3 - r_2) \cos \alpha} \right| \quad (2.22)$$

and its dimensionless form

$$\bar{\epsilon}_3 = \left| \ln \frac{1 - r_P^* + \rho_P^* s_0^* - s_0^* (\rho_P^* + \rho_D^* + 1) \sin \alpha}{(r_3^* - r_2^*) \cos \alpha} \right| \quad (2.23)$$

Thus, the deformation energy becomes

$$W_3 = W_s(\bar{\epsilon}_3) \cdot \pi(r_3^2 - r_2^2) s_0 \quad (2.24)$$

and its dimensionless

$$W_3^* = W_s^*(\bar{\epsilon}_3) \cdot (r_3^{*2} - r_2^{*2}) \quad (2.25)$$

2.2.4 Area 4

In this area, the strain is similar as that in Area 2. Assuming ϵ_α being uniform gives

$$\epsilon_{\alpha 4} = \ln \frac{\alpha \rho_2}{r_4 - r_3} \quad (2.26)$$

or

$$\epsilon_{\alpha 4} = \ln \frac{\alpha \rho_2^* \rho_D^* s_0^*}{r_4^* - r_3^*} \quad (2.27)$$

The circumferential strains in section C and D are

$$\epsilon_{\varphi C} = \ln \frac{r_i - \rho_2 \sin \alpha}{r_3} \quad (2.28)$$

and

$$\epsilon_{\varphi D} = \ln \frac{r_i}{r_4} \quad (2.29)$$

Taking the mean value of $\epsilon_{\varphi C}$ and $\epsilon_{\varphi D}$ gives the circumferential strain in this area

$$\epsilon_{\varphi 4} = \frac{1}{2} \ln \frac{r_i^2 - r_i \rho_2 \sin \alpha}{r_3 r_4} \quad (2.30)$$

or, its dimensionless is

$$\epsilon_{\varphi 4} = \frac{1}{2} \ln \frac{1 - s_0^* \rho_2^* \rho_D^* \sin \alpha}{r_3^* r_4^*} \quad (2.31)$$

Thus, the total effective strain is

$$\bar{\epsilon}_4 = \frac{2}{\sqrt{3}} \cdot \sqrt{\epsilon_{\alpha 4}^2 + \epsilon_{\varphi 4}^2 + \epsilon_{\alpha 4} \cdot \epsilon_{\varphi 4}} \quad (2.32)$$

The deformation energy of this area is

$$W_4 = \int W_s(\bar{\epsilon}_4) dv \quad (2.33)$$

where the volume element (see Appendix B)

$$dv = \rho_2(\alpha r_1 - 2\rho_2 \sin^2 \frac{\alpha}{2}) \cdot d\rho_2 \quad (2.34)$$

To ensure volume invariance, this integration of Eq.(2.33) must take place over the current thickness of the sheet s_4 , that is,

$$W_4 = \int_{\rho_D}^{\rho_D + s_4} W_s(\bar{\epsilon}_4) \cdot \rho_2(\alpha r_1 - 2\rho_2 \sin^2 \frac{\alpha}{2}) \cdot d\rho_2 \quad (2.35)$$

and the dimensionless gives

$$W_4^* = 2\rho_D^* s_0^* \int_1^{1 + \frac{s_4^*}{\rho_D^*}} W_s^*(\bar{\epsilon}_4) \cdot \rho_2^* \left(\frac{\alpha}{\rho_D^* s_0^*} - 2\rho_2^* \sin^2 \frac{\alpha}{2} \right) \cdot d\rho_2^* \quad (2.36)$$

where the upper limitation of this integration $1 + \frac{s_4^*}{\rho_D^*}$ is determined in Appendix B.

2.2.5 Area 5

In this area, assuming the flange remains plane-parallel during deformation and applying volume invariance gives

$$(r_{u0}^2 - r_4^2) s_0 = (r_u^2 - r_1^2) s \quad (2.37)$$

where s is the mean thickness of this area. Neglecting the blankholder force and friction forces implies a uniaxial stress condition at $r=r_u$, it then follows

$$\frac{s}{s_0} = \sqrt{\frac{r_{u0}}{r_u}} \quad (2.38)$$

Eliminating s from Eqs.(3.37) and (3.38) gives an implicit relation for r_u

$$r_{u0}^2 - r_4^2 = (r_u^2 - r_1^2) \sqrt{\frac{r_{u0}}{r_u}} \quad (2.39)$$

quoted $\beta = \frac{r_u}{r_i}$, its dimensionless becomes

$$(\beta^2 - 1) \sqrt{\frac{\beta_0}{\beta}} = \beta_0^2 - r_4^{*2} \quad (2.40)$$

The circumferential strain is

$$\epsilon_\varphi = \ln \frac{r}{r_0} = \ln \frac{r^*}{r_0^*} \quad (2.41)$$

where r_0 is the initial local radius. With volume invariance it follows

$$(r_0^2 - r_4^2) s_0 = (r^2 - r_4^2) s \quad (2.42)$$

and with Eq.(2.38)

$$r_0^{*2} = (r^{*2} - 1) \sqrt{\frac{\beta_0}{\beta}} + r_4^{*2} \quad (2.43)$$

Thus, substitution of Eq.(2.43) into (2.41) gives

$$\epsilon_\varphi = \frac{1}{2} \ln \frac{r^{*2}}{(r^{*2} - 1) \sqrt{\frac{\beta_0}{\beta}} + r_4^{*2}} \quad (2.44)$$

The strain in z -direction is

$$\epsilon_z = \ln \frac{s}{s_0} = \frac{1}{2} \ln \frac{\beta_0}{\beta} \quad (2.45)$$

With Eqs.(2.44) and (2.45), the effective strain yields

$$\bar{\epsilon}_5 = \frac{2}{\sqrt{3}} \cdot \sqrt{\epsilon_\varphi^2 + \epsilon_z^2 + \epsilon_\varphi \cdot \epsilon_z} \quad (2.46)$$

Therefore, the deformation energy comes

$$W_5 = \int_{r_i}^{r_u} W_s(\bar{\epsilon}_5) \cdot 2\pi r s \cdot dr \quad (2.47)$$

and its dimensionless is

$$W_5^* = 2 \sqrt{\frac{\beta_0}{\beta}} \int_1^\beta W_s^*(\bar{\epsilon}_5) \cdot r^* \cdot dr^* \quad (2.48)$$

So far, the deformation energy in the whole sheet, a sum of the energy in the bottom region Area 1, in two bending regions Area 2 and Area 4, in the stretching region Area 3

and in the flange region Area 5, is obtained, that is,

$$W^* = W_1^* + W_2^* + W_3^* + W_4^* + W_5^* \quad (2.49)$$

III. RESULTS AND CONCLUSIONS

In the graphs given below the results are shown of the numerical optimization of the total energy W^* with respect to the free parameters r_1^* , r_2^* , r_3^* , and r_4^* .

The calculations were carried out using the following input:

$$\beta_0 = 1.8, 2.1, \text{ and } 2.4 \text{ respectively;}$$

$$s_0 = 1 \text{ mm;}$$

$$r_p = 30 \text{ mm;}$$

$$\rho_p = \rho_d = 5 \text{ mm;}$$

$$t = 1.15 \text{ mm;}$$

$$r_{u0} = \beta_0(30+1.15+5) \text{ mm.}$$

In Fig.3.1 the total dimensionless deformation energy is given as a function of the parameter α , where Fig.3.2 a until 3.2 c show the change of the free parameters with the increasing α . The change of these quantities is as one expects.

More interesting are the results in Fig.3.3 a until 3.3 c where the continuous increasing value of the strain of the middle plane(measured along the contour) in all the areas is shown, where the strain of area 5 concerns the value at $r=r_i$.

In Fig.3.4, a comparison is made between the average effective strain of the middle plane of this analysis and of a FEM approach[1].

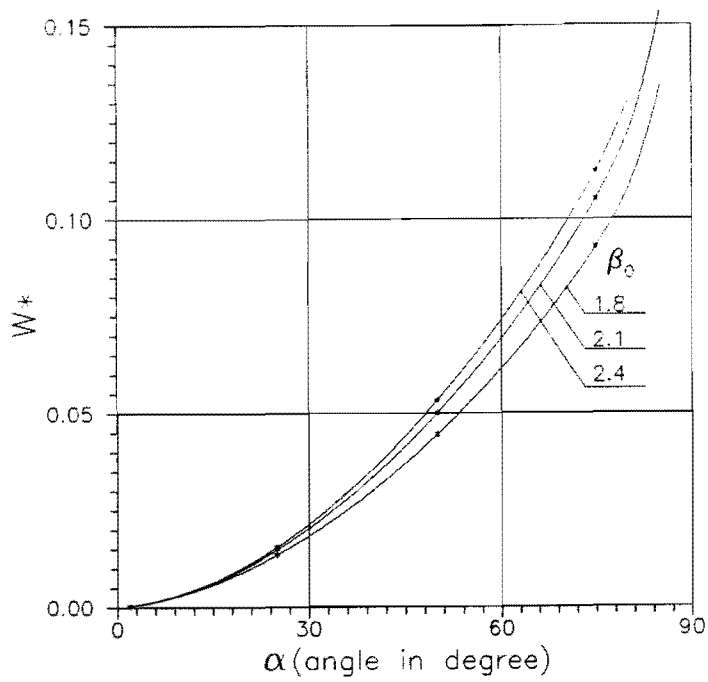


Fig.3.1 The Deformation Energy

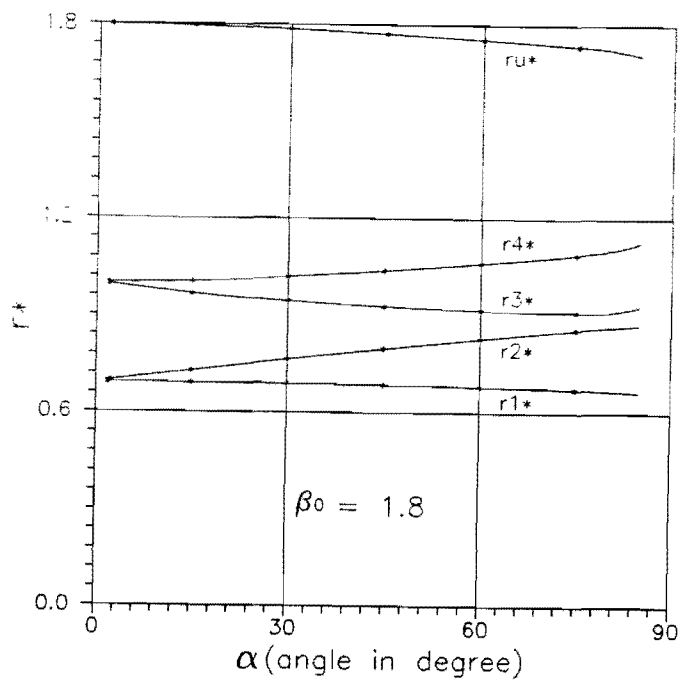


Fig.3.2 a The Initial Position ($\beta_0=1.8$)

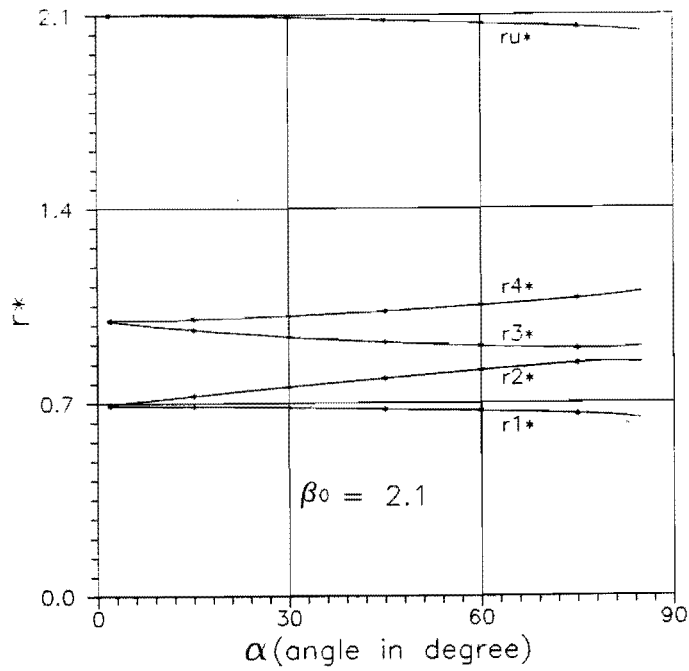


Fig.3.2 b The Initial Position ($\beta_0=2.1$)

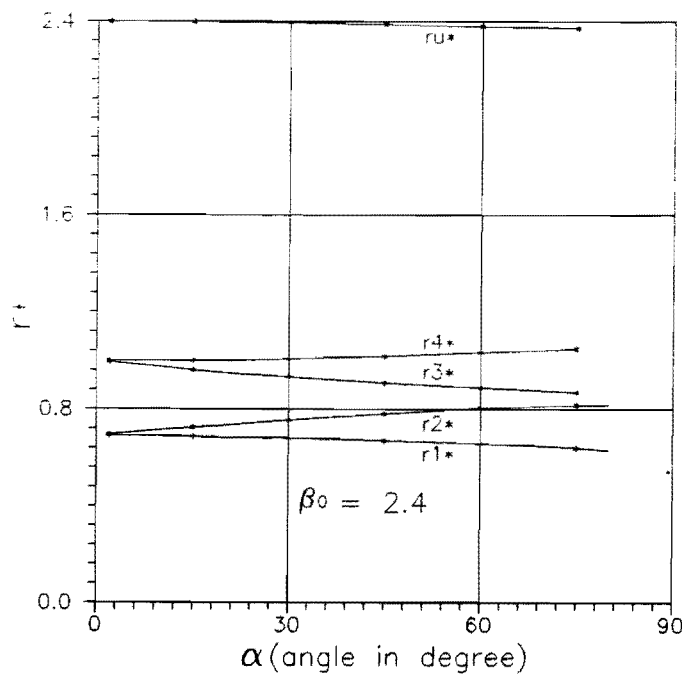


Fig.3.2 c The Initial Position ($\beta_0=2.4$)

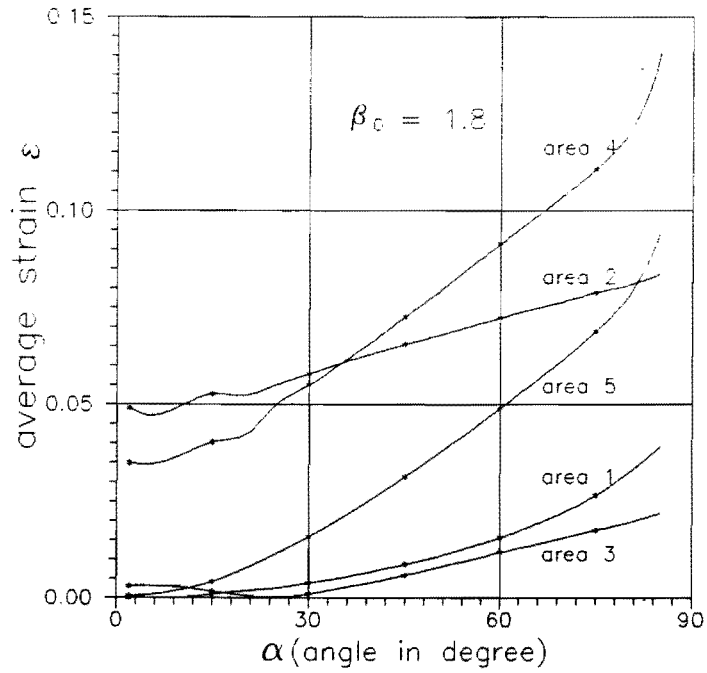


Fig.3.3 a The Average Radial Strains ($\beta_0=1.8$)

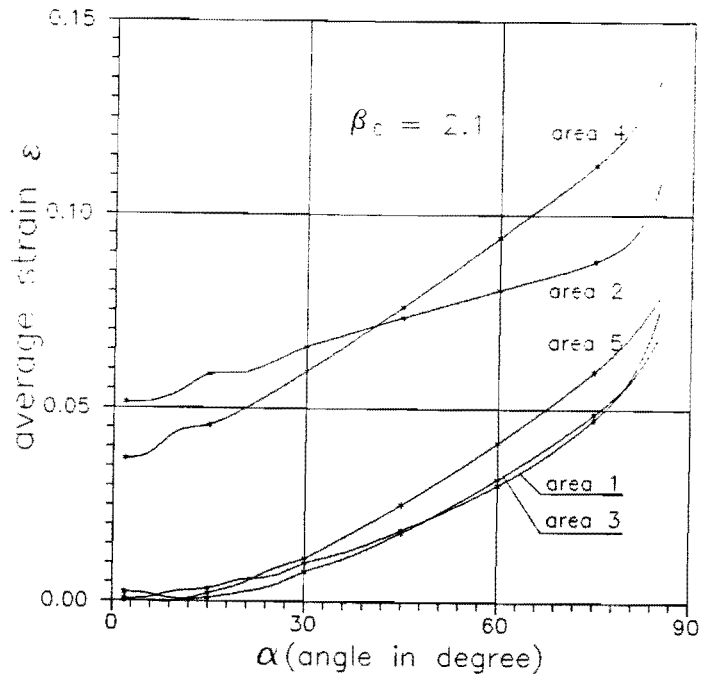


Fig.3.3 b The Average Radial Strains ($\beta_0=2.1$)

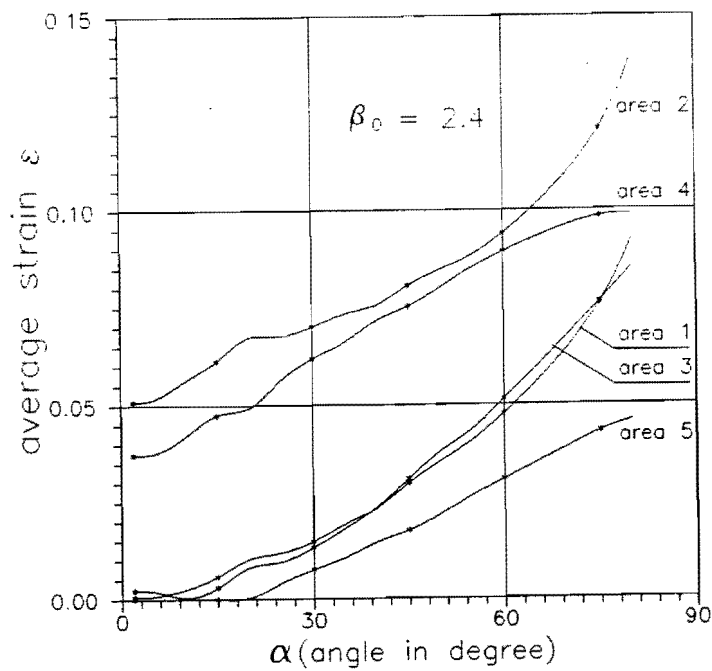


Fig.3.3 c The Average Radial Strains ($\beta_0=2.4$)

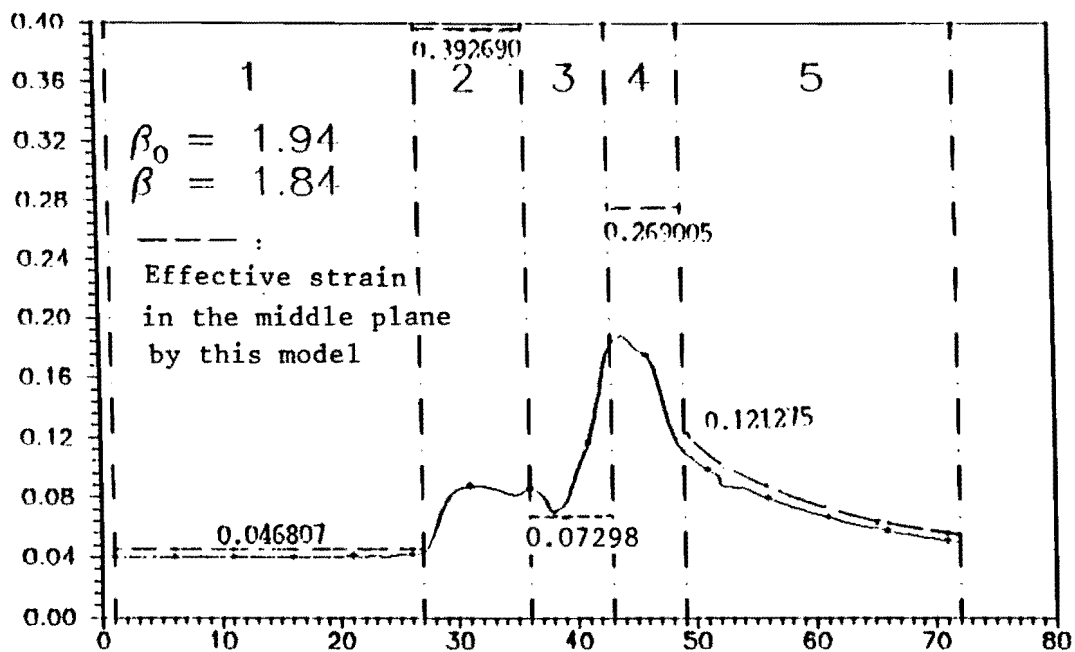


Fig.3.4 Comparison between This Analysis and FEM

On the basis of these results the following preliminary conclusions can be drawn:

___ It is obvious that in the very beginning of the deep-drawing process the "stiffness" in the stretch-bending areas (2 and 4) is much smaller than that in other zones where just stretching or compression takes place. The results in Fig.3.4 clearly shows this effect.

___ With respect to area 1, 3 and 5 there is good agreement between the analysis of this report and the FEM. This means that the applied modelling in these areas, especially 1 and 5, is rather good.

However, the difference in area 2 and 4 between both this analysis and FEM is substantial, the ones of this report probably far too high.

Thus on the whole the results so far are not satisfactory, especially considering the fact that the aim of the analysis was to predict something about the critical deep-drawing ratio β_0 which appears to be directly related to the stretch-bending process in area 2.

___ The extend of the approximation of the straight strain path is not clear. A more complete description of the process could be established by applying an incremental analysis involving the calculation of the strain history of the material in a proper way. However the analysis in that case will be much more complicated and the computation time relatively high (now about 40 hours on a AT486).

___ The use of the standard program *MINIFUN* for these kinds of optimization problems, where in general the functions are very flat, becomes in view of other experiences more and more questionable. Whether this is due to the problem itself or to the fact that there is more in it than we got out of it, is not very clear. More study on

this subject thoroughly is necessary.

APPENDIX

A. Derivation of u

The displacement of the punch u is (see Fig.A.A).

$$u = a_1 + a_2 + a_3 \tag{ A.A.1}$$

where

$$a_1 = \rho_D(1 - \cos \alpha)$$

$$a_2 = [r_i - r_P + \rho_P - (\rho_P + \rho_D + s_0) \sin \alpha] \cdot \tan \alpha$$

$$a_3 = (\rho_P + s_0)(1 - \cos \alpha)$$

and α is the angle containing the arc of the fillet of the punch or the die contacted with the sheet.

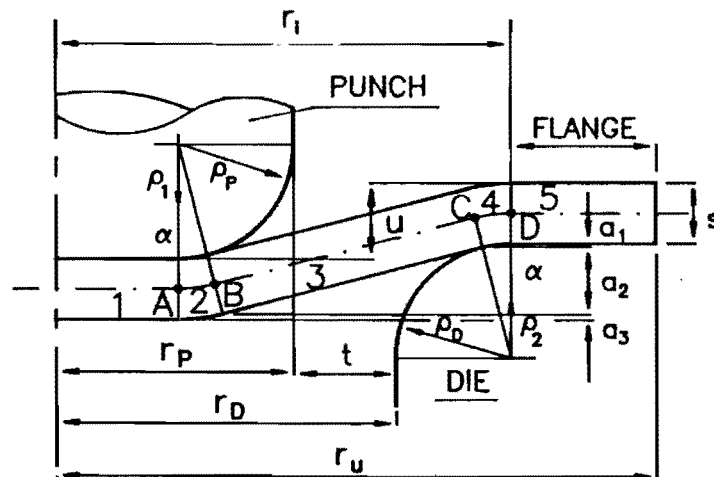


Fig.A.A

B. Derivations of dv , $1 + \frac{s_2^*}{\rho_P^*}$, and $1 + \frac{s_4^*}{\rho_D^*}$

1. About dv in Area 2 (see Fig.A.B.a)

From the rule of Guldin, it follows

$$dv = 2\pi(r_P - \rho_P + \rho_z \sin \frac{\pi}{2}) \alpha \rho_1 d\rho_1 \tag{A.B.1}$$

where ρ_z is the position of the centre of gravity of the considered section, it is

$$\begin{aligned} \rho_z &= \rho_1 \cdot \frac{2\rho_1 \sin(\alpha/2)}{\alpha \rho_1} \\ &= \frac{2\rho_1 \sin(\alpha/2)}{\alpha} \end{aligned} \tag{A.B.2}$$

thus,

$$dv = 2\pi[\alpha(r_P - \rho_P) + 2\rho_1 \sin^2 \frac{\pi}{2}] \cdot \rho_1 d\rho_1 \tag{A.B.3}$$

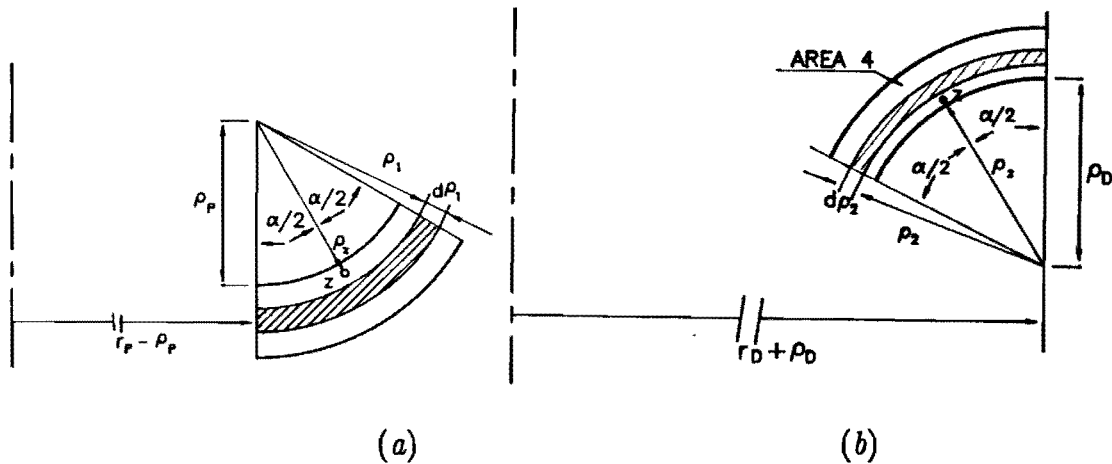


Fig.A.B

2. About $1 + \frac{s_2^*}{\rho_P^*}$ in Area 2

Volume invariance yields to

$$\pi(r_2^2-r_1^2)s_0=2\pi\int_{\rho_P}^{\rho_P+s_2} [\alpha(r_P-\rho_P)+2\rho_1\sin^2\frac{\pi}{2}]\cdot\rho_1d\rho_1 \quad (\text{A.B.4})$$

It gives the equation

$$\begin{aligned} \frac{1}{2}(r_2^2-r_1^2)s_0 &= \frac{\pi}{2}(r_P-\rho_P)(\rho_P+s_2)^2 + \frac{2}{3}\sin^2\frac{\alpha}{2}(\rho_P+s_2)^3 - \\ &- \frac{\alpha}{2}(r_P-\rho_P)\rho_P^2 - \frac{2}{3}\sin^2\frac{\alpha}{2}\cdot\rho_P^3 \end{aligned} \quad (\text{A.B.5})$$

and its dimensionless can be rewritten

$$\begin{aligned} \frac{2}{3}\sin^2\frac{\alpha}{2}\cdot\left(1+\frac{s_2^*}{\rho_P^*}\right)^3 + \frac{\alpha}{2}\left(\frac{r_P^*}{\rho_P^*s_0^*}-1\right)\left(1+\frac{s_2^*}{\rho_P^*}\right)^2 - \\ - 0.5\frac{r_2^{*2}-r_1^{*2}}{\rho_P^{*3}\cdot s_0^{*2}} - \frac{\alpha}{2}\left(\frac{r_P^*}{\rho_P^*s_0^*}-1\right) - \frac{2}{3}\sin^2\frac{\alpha}{2} = 0 \end{aligned} \quad (\text{A.B.6})$$

This equation is regarded as the following

$$A\cdot X^3+B\cdot X^2+C=0 \quad (\text{A.B.7})$$

which is the equation with the unknown parameter $X=1+\frac{s_2^*}{\rho_P^*}$ that is the upper

limitation of the integral of (2.21), and where

$$A = \frac{2}{3}\sin^2\frac{\alpha}{2} \quad (\text{A.B.8})$$

$$B = \frac{\alpha}{2}\left(\frac{r_P^*}{\rho_P^*s_0^*}-1\right) \quad (\text{A.B.9})$$

$$C = -0.5\frac{r_2^{*2}-r_1^{*2}}{\rho_P^{*3}\cdot s_0^{*2}} - \frac{\alpha}{2}\left(\frac{r_P^*}{\rho_P^*s_0^*}-1\right) - \frac{2}{3}\sin^2\frac{\alpha}{2} \quad (\text{A.B.10})$$

3. About dv in Area 4 (see Fig.A.B.b)

Similar to the derivation of [B.1] above, it follows

$$dv = 2\pi\rho_2\left(\alpha r_i - 2\rho_2\sin^2\frac{\alpha}{2}\right)\cdot d\rho_2 \quad (\text{A.B.11})$$

4. About $1 + \frac{s_4^*}{\rho_D^*}$ in Area 4

Volume invariance in this area gives the equation

$$\pi(r_4^2 - r_3^2)s_0 = 2\pi \int_{\rho_D}^{\rho_D + s_4} (\alpha r_1 - 2\rho_2 \sin^2 \frac{\alpha}{2}) \cdot \rho_2 d\rho_2 \quad (\text{A.B.12})$$

that is,

$$\begin{aligned} & \frac{2}{3} \sin^2 \frac{\alpha}{2} \cdot \left(1 + \frac{s_4^*}{\rho_D^*}\right)^3 + \frac{\alpha}{2} \cdot \frac{1}{\rho_D^* s_0^*} \left(1 + \frac{s_4^*}{\rho_D^*}\right)^2 + \\ & + 0.5 \frac{r_4^{*2} - r_3^{*2}}{\rho_D^{*3} \cdot s_0^{*2}} + \frac{\alpha}{2} \cdot \frac{1}{\rho_D^* s_0^*} - \frac{2}{3} \sin^2 \frac{\alpha}{2} = 0 \end{aligned} \quad (\text{A.B.13})$$

Similar to Eq.(A.B.7), this equation contains unknown parameter $X = 1 + \frac{s_4^*}{\rho_D^*}$, which is needed for the upper limitation of the integral (2.36), with the coefficients

$$\begin{aligned} A &= \frac{2}{3} \sin^2 \frac{\alpha}{2} & B &= \frac{\alpha}{2} \cdot \frac{1}{\rho_D^* s_0^*} \\ C &= 0.5 \frac{r_4^{*2} - r_3^{*2}}{\rho_D^{*3} \cdot s_0^{*2}} + \frac{\alpha}{2} \cdot \frac{1}{\rho_D^* s_0^*} - \frac{2}{3} \sin^2 \frac{\alpha}{2} \end{aligned}$$

C. Uniaxial Stress in Region 3

Because of equilibrium in the 2-direction (see Fig.A.C) σ_3 must be zero. So there is uniaxial stress in the 1-direction.

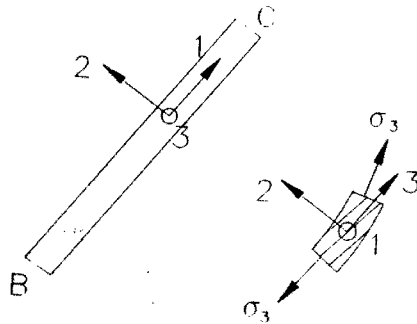


Fig.A.C